

Enzyme-Induced Staining of Biomembranes with Voltage-Sensitive Fluorescent Dyes

Marlon J. Hinner, Gerd Hübener, and Peter Fromherz*

Department of Membrane and Neurophysics, Max Planck Institute for Biochemistry, Martinsried/München, Germany 82152

Received: September 19, 2003; In Final Form: November 22, 2003

We consider the physicochemical basis for enzyme-induced staining of cell membranes by fluorescent voltage-sensitive dyes, a method that may lead to selective labeling of genetically encoded nerve cells in brain for studies of neuronal signal processing. The approach relies on the induction of membrane binding by enzymatic conversion of a water-soluble precursor dye. We synthesized an amphiphilic hemicyanine dye with and without an additional phosphate appendix at its polar headgroup. The fluorescence of these dyes is negligible in water but high when bound to lipid membranes. By fluorescence titration with lipid vesicles it was shown that the phosphate group lowers the partition coefficient from water to membrane by more than an order of magnitude. By isothermal titration calorimetry, we showed that the dye phosphate was a substrate for a water-soluble alkaline phosphatase following Michaelis–Menten kinetics. In a suspension of lipid vesicles, the enzyme reaction led to a fluorescence increase due to enhanced membrane binding of the product dye in accord with the Michaelis–Menten kinetics of the reaction and the partition coefficients of substrate and product. We successfully tested the staining method by fluorescence microscopy with individual giant lipid vesicles and with individual red blood cells. In both systems, the membrane fluorescence due to bound hemicyanine was enhanced by an order of magnitude, proving the feasibility of enzyme-induced staining with voltage-sensitive dyes.

Introduction

Voltage-sensitive fluorescent dyes are well-established probes for optical recording of voltage transients in nerve membranes. Since their first application in 1968¹ and their further development in the following decades,^{2–10} they have been successfully used in cultured nerve cells and in nerve tissue.^{11–13} Optical recording allows the study of neurons and brain at a high temporal and spatial resolution.

Common extracellular application of the dyes leads to staining of all cells in a tissue. As a consequence, voltage transients of individual neurons cannot be measured. Significant progress would be achieved if a satisfactory method for selective staining of individual neurons or groups of neurons were available. So far, intracellular application of dyes has been considered.^{14,15} With this method, however, also intracellular structures are stained with the concomitant effects of background fluorescence and phototoxicity. In addition, slow intracellular diffusion may lead to incomplete staining. Attempts using genetically encoded fluorescent proteins with intrinsic voltage sensitivity have had modest success hitherto.^{16,17}

We envisage a cell-selective staining that relies on extracellular application of an organic precursor dye and its local activation at a selected cell by a genetically encoded enzyme. Such an activation could rely on an induction of fluorescence quantum yield, voltage sensitivity, or induction of the interaction with the membrane. The latter approach is particularly attractive because the crucial chemical structure of the voltage-sensitive chromophore would not be affected by enzymatic activation. In our vision shown in Figure 1, a nerve cell in brain tissue is genetically induced to express a membrane-bound enzyme with its active site facing the extracellular space. That

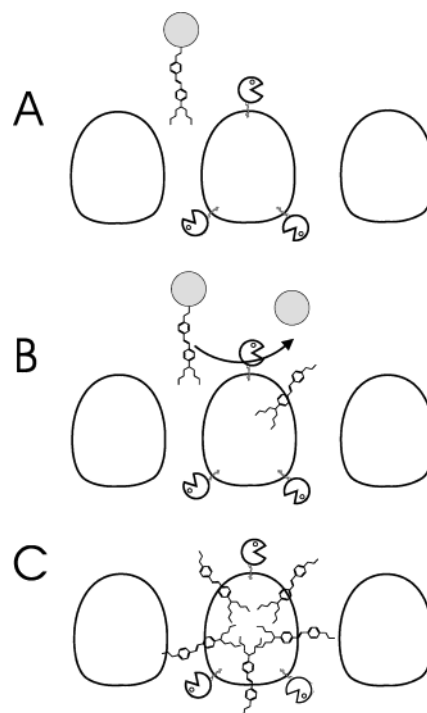


Figure 1. Concept for enzyme-induced selective staining of cells. (A) The two components are a voltage-sensitive dye derivatized with an enzymatically cleavable appendix to the polar headgroup (represented by a circle) and an ectoenzyme expressed on the surface of a selected cell in a tissue symbolized by three cells. (B) The dye is hydrolyzed by the ectoenzyme. Upon cleavage of the appendix, the dye binds to the membrane. (C) Cleaved dye accumulates in the membrane of that cell where it was produced.

* Address correspondence to this author. Phone: +49 89 8578 2820. Fax: +49 89 8578 2822. E-mail: fromherz@biochem.mpg.de.

ectoenzyme cleaves off a polar group of a water-soluble precursor dye such that the overall lipophilicity of the dye is

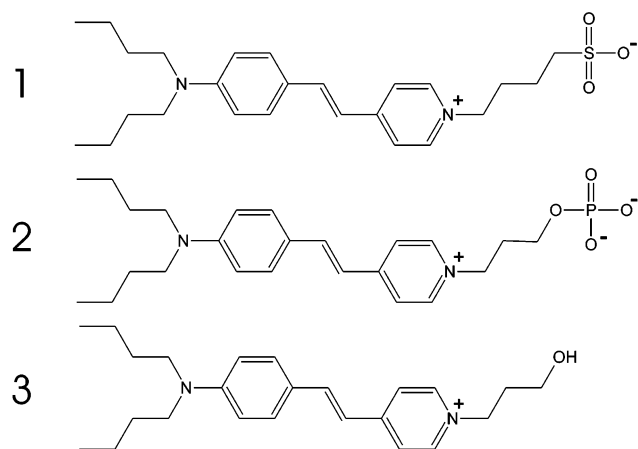


Figure 2. Voltage-sensitive hemicyanine dyes of the dibutylamino-styrylpyridinium (Di-4-ASP) type: (1) the common Di-4-ASP butylsulfonate (Di-4-ASPBS), (2) the substrate of enzyme activation Di-4-ASP propyl phosphate (Di-4-ASPPP), and (3) the product of enzyme activation Di-4-ASP propyl alcohol (Di-4-ASPPA).

enhanced. As a consequence, the voltage-sensitive dye binds to the adjacent cell membrane.

In the present paper, we explore basic physicochemical problems of induced membrane binding of a voltage-sensitive dye using a water-soluble enzyme. In the test system we studied a modified styryl hemicyanine Di-4-ASPBS⁶ (Figure 2, dye 1), with its sulfonate headgroup replaced by a phosphate group (dye 2, Di-4-ASPP phosphate). Hydrolysis of Di-4-ASPP phosphate leads to Di-4-ASPP alcohol (Figure 2, dye 3). The phosphate was chosen for two reasons: (i) It has a high polarity due to its two negative charges in moderately alkaline solution, with acidity constants of phosphate monoesters being $pK_{a1} \approx 1$ and $pK_{a2} \approx 6$.¹⁸ (ii) Activation relies on alkaline phosphatase, an enzyme with a broad range of substrate specificity.¹⁹ At first we characterized the partition coefficient of the dyes between water and membrane in suspensions of liposomes. Then, the cleavage of the phosphate appendix by alkaline phosphatase from the human placenta (PLAP) was studied by liquid chromatography and isothermal titration calorimetry. Combining these two elements, enzyme-induced binding was implemented with liposomes. Finally the staining method was tested with individual giant lipid vesicles and red blood cells.

Materials and Methods

Chemicals. The purity of all chemicals other than those used for synthesis was at least p.a.: TRIS (Roth, Karlsruhe, Germany), acetonitrile (YMC Europe, Schermbeck, Germany), Sephadex LH20 (Pharmacia, Peapack, NJ), $ZnSO_4 \cdot 7H_2O$, $CaCl_2 \cdot 2H_2O$, trichloromethane, methanol, CH_3COOH , diethyl ether, silica gel 60 (0.040–0.063 mm), iodine, $MgCl_2 \cdot 6H_2O$, trifluoroacetic acid (TFA), saccharose, (Merck, Darmstadt, Germany), dimethylchlorophosphate (Aldrich, Munich, Germany), diethanolamine (DEA), *p*-nitrophenyl phosphate (*p*-NPP), 1-bromopropanol, pyridine, dimethyl sulfide, phosphoric acid (Fluka, Munich, Germany), KCl, NaCl, poly-L-lysine MW 150000–300000 (Sigma, Munich, Germany). Purified water was obtained with a Milli-Q system (Millipore Germany, Schwalbach).

Dye. Di-4-ASPBS was synthesized as described in the literature.²⁰ Di-4-ASPP alcohol (1-[γ -hydroxypropyl]-*trans*-4-[*p*-(di-*n*-butylamino)styryl]pyridinium bromide) was obtained by reaction of *trans*-4-[*p*-(di-*n*-butylamino)styryl]pyridine (Di-4-ASP) with 1.5 mol equiv of 1-bromopropanol (100 °C, 2 h).

Subsequent precipitation of the product from methanol with diethyl ether and digestion in ethyl acetate yielded Di-ASPP alcohol as a red solid. It was purified by column chromatography (SiO_2 , $CHCl_3$:MeOH:H₂O 50:20:4) and identified by NMR and mass spectrometry: ¹H NMR (400 MHz, $CDCl_3$) δ ppm 8.97 (d, 2H, ³*J* = 5.2 Hz), 7.785 (d, 2H, ³*J* = 5.2 Hz), 7.58 (d, 1H, ³*J* = 15.6 Hz), 7.48 (d, 2H, ³*J* = 7.8 Hz), 6.81 (d, 1H, ³*J* = 15.6 Hz), 6.62 (d, 2H, ³*J* = 7.8 Hz), 4.80 (m, br, 2H), 4.44 (s, br, 1H), 3.71 (t, 2H, ³*J* = 5.0 Hz), 3.32 (s, br, 4H), 2.27 (t, 2H, ³*J* = 5.0 Hz), 1.58 (m, br, 4 Hz), 1.36 (q, 4H, ³*J* = 7.0 Hz), 0.96 (t, 6H, ³*J* = 7.0 Hz); EIMS *m/z* 367.2 M⁺ ($C_{24}H_{35}N_2O^+$ requires 367.6).

The first step of the synthesis of Di-ASPP phosphate (1-[γ -phosphatopropyl]-*trans*-4-[*p*-(di-*n*-butylamino)styryl]pyridinium betaine) leads to Di-4-ASPP dimethyl phosphate by reaction of Di-4-ASPP alcohol with 1.6 mol equiv of dimethylchlorophosphate in pyridine (16 h, room temperature). After evaporation of the solvent, the red intermediate product was purified by chromatography on a silica column ($CHCl_3$:MeOH:H₂O 60:20:1). The phosphate was deprotected with 5 mol equiv of dimethyl sulfide and 17 mol equiv of methanesulfonic acid and stirring overnight at room temperature. Upon neutralization with 25% NH₃, the colorless solution turned red. After evaporation, the red product was purified by column chromatography (SiO_2 , $CHCl_3$:MeOH:H₂O 50:20:4; Sephadex LH 20, MeOH). It was identified by NMR and mass spectrometry: ¹H NMR (400 MHz, MeCN) δ 8.60 (s, br, 2H), 7.72 (s, br, 2H), 7.50 (d, 1H, ³*J* = 15.5 Hz), 7.355 (d, 2H, ³*J* = 7.8 Hz), 6.71 (d, 1H, ³*J* = 15.5 Hz), 6.51 (d, 2H, ³*J* = 7.8 Hz), 4.525 (s, br, 2H), 3.925 (s, br, 2H), 3.20 (s, br, 6H, O-*H*, N-*CH*₂), 2.17 (s, br, 2H), 1.445 (s, br, 4H), 1.26 (m, 4H), 0.87 ppm (t, 6H, ³*J* = 7.2 Hz); ³¹P NMR (162 MHz, $CDCl_3$) δ 4.59 ppm; EIMS *m/z* 447.2 M⁺ ($C_{24}H_{36}N_2O_4P^+$ requires 447.5).

The absorption maximum of Di-4-ASPP alcohol in Tris-NaCl buffer (20 mM Tris, 100 mM NaCl, pH 8.1) was at 482 nm with an extinction coefficient of 3.91×10^4 M⁻¹ cm⁻¹ (Varian Cary 3E spectrometer, Mulgrave, Victoria, Australia). For Di-4-ASPP phosphate (FW = 447.5) in the same buffer we found an extinction coefficient of 3.40×10^4 M⁻¹ cm⁻¹ at 479 nm. According to NMR data the preparation contained no organic impurities. Our elementary analysis was in good agreement with the assumption that Di-4-ASPP phosphate contained 4 water molecules per dye, where we found C 55.8% (55.6% expected for Di-4-ASPP phosphate·4H₂O), H 8.2% (8.4%), N 5.5% (5.6%), P 5.7% (6.0%). For Di-4-ASPP phosphate·4H₂O (FW = 519.5), the extinction coefficient corresponds to 3.95×10^4 M⁻¹ cm⁻¹. Solutions of defined concentration were prepared assuming the extinction coefficients of the dyes to be equal.

Fluorescence measurements were performed with an SLM Aminco 8100 fluorescence spectrometer (Acton Research, Acton, MA), using an avalanche photodiode in the detection channel (Polytec, Waldbronn, Germany). The bandwidths for excitation and emission were 16 and 36 nm, respectively. All measurements were performed under magic angle conditions. This was done to exclude possible effects of lifetime-dependent spectra on the detected signal due to common polarization in the excitation and emission monochromator. The cuvette holder was kept at a temperature of 25 °C (LAUDA RM 6 Thermostat). The maxima of fluorescence excitation and emission in Tris-NaCl buffer were around 490 and 630 nm for both dyes. For dye bound to POPC membranes (Tris-NaCl, 10 mM POPC vesicles), the excitation maxima were shifted to around 475 (Di-4-ASPP alcohol) and 465 nm (Di-4-ASPP phosphate) and the emission of both dyes was shifted to 600 nm.

Dye-Lipid Binding. The binding of the dyes to lipid membranes was determined by fluorescence lipid titration²¹ with large unilamellar vesicles (LUVs) made of 1-palmitoyl-2-oleoyl-phosphatidylcholine (POPC). The lipid was purchased from Avanti Polar Lipids (Alabaster, AL), Lipoid KG (Ludwigshafen, Germany), and Matreya (State College, PA). The purity of the lipids was checked by 2-dimensional TLC.²² The vesicles were made by extrusion²³ in Tris-NaCl buffer (20 mM Tris, 100 mM NaCl, pH 8.1), using an extrusion apparatus and polycarbonate filters with 100 nm pore size (both Avestin Europe, Mannheim, Germany). Vesicle size was determined by quasielastic light scattering, using an argon ion laser (Spectra-Physics, Darmstadt, Germany), a photomultiplier (Brookhaven Instruments, Vienna, Austria), and a correlator (ALV-5000, Langen, Germany). The lipid concentration was determined by a chromogenic enzyme assay (Biomerieux, Marcy l'Etoile, France). The standard deviation of three concentration measurements for every vesicle preparation was always below 4%. Vesicles were stored under argon at 4 °C in 15-mL Falcon Centrifuge Tubes (BD Labware Europe, Le Pont de Claix, France) and used within 3 days.

To measure dye binding constants, we prepared 1 mM solutions of the dyes 1–3 by ultrasonication in ethanol (1) or Tris-NaCl buffer (2 and 3). These stock solutions were diluted in Tris-NaCl buffer to a concentration of 1 μ M. In the same buffer, suspensions of POPC vesicles with concentrations ranging from 100 nM to 10 mM were prepared by dilution of stock solutions. Dye and lipid were prethermostated to 25 °C. Equal volumes of both were mixed directly before measurement. The fluorescence emission recorded at 600 nm with excitation at 488 nm was used for the evaluation of the partition coefficients.

Enzyme. We used HPLC to determine whether Di-4-ASPP phosphate is a substrate for alkaline phosphatase from the Human Placenta (PLAP). The activity of the two batches of the enzyme (Sigma) was tested with 1 mM *p*-NPP ($\epsilon = 18.5 \times 10^3 \text{ M}^{-1} \text{ cm}^{-1}$) as a chromogenic substrate in DEA buffer (1 M DEA, 1 mM MgCl_2 and 10 μ M ZnSO_4 , pH 9.8) at 37.0 ± 0.3 °C. The activities obtained were 27.2 ± 0.4 Units/mg and 26.1 ± 0.5 Units/mg (a Unit is defined as the activity necessary to digest 1 μ M *p*-NPP per minute). The purity of the samples was tested by liquid chromatography coupled with mass spectrometry (LCMS; Sciex API 165, Perkin-Elmer Instruments, Rodgau-Jügesheim, Germany) with a Nucleosil-100-5 C8 column (Macherey & Nagel, Düren, Germany; solution A: 0.05% TFA in H_2O ; solution B: 0.05% TFA in acetonitrile; gradient: 80% H_2O to 10% H_2O in 15 min). It was found that for both batches the elution profile was identical, and that both contained a mixture of various compounds not further identified. The impurity of commercially available PLAP is documented in the literature.²⁴ Since the activity per milligram varies between the batches, we refer all concentrations and activities to DEA Units, i.e., the activity that an equal amount of PLAP would have in DEA buffer (pH 9.8, 37 °C).

In the HPLC assay, Tris-NaCl buffer containing 55 μ M dye and 0.24 DEA Units/mL of PLAP was incubated for 3 h at room temperature. The enzyme was separated by filtering through a Centricon YM-3 membrane (Millipore, Billerica, MA) with a cutoff at 3 kD. The filtered solution was concentrated to dryness in a vacuum centrifuge at room temperature. The analytes were dissolved in acetonitrile/ H_2O (1:1) and HPLC analysis (Bischoff, Leonberg, Germany) was performed with a C18 Nucleosil column (100-7, Macherey & Nagel, Düren, Germany) and 10 mM phosphoric acid and acetonitrile as eluents

(gradient 30% to 70% phosphoric acid in 15 min) with optical detection at 533 nm.

Enzyme Kinetics with ITC. We performed enzyme kinetic measurements with Di-4-ASPP phosphate as a substrate of PLAP by isothermal titration calorimetry (ITC). We used Tris-NaCl buffer (20 mM Tris, 100 mM NaCl, pH 8.1) without Zn^{2+} and Mg^{2+} although most alkaline phosphatases depend on these metals for maximum activity. However, divalent cations bind to lipid membranes and induce their aggregation and fusion.²⁵ The pH value is a compromise between optimal enzymatic activity (at pH 9.8) and compatibility with vesicles and cells. The microcalorimeter (VP-ITC, Microcal, Northampton, MA) was thermostated to 25.0 °C, with reference power set to 10 μ cal/s and a stirring speed of 310 rpm. The sample cell contained a PLAP solution of 0.19 DEA Units/mL activity and the syringe was filled with a 1 mM solution of Di-4-ASPP phosphate. The reference cell contained buffer only. Different amounts of dye were injected into the sample cell in separate experiments to cover a concentration range from 2 to 15 μ M. To determine the heats of dilution alone, injections were carried out with pure buffer. For both hydrolysis and dilution, the baseline signal was approximated by linear or polynomial functions and subtracted from the raw signal resulting in a curve with a flat baseline. The dilution signal was subtracted from the signal of the enzymatic reaction to yield the final calorimeter tracing of enzymatic hydrolysis. The molar heat of reaction was obtained by integration. The initial velocities were determined from the average heat of reaction of the first 10 to 30 s after the onset of the reaction, using the mean molar heat of reaction as a proportionality constant. Data analysis, including estimates of statistical errors of nonlinear curve fits, was performed with Origin (OriginLab Software, Northampton, MA).

Sucrose-Loaded Vesicle-Binding Assay. This assay²⁶ was used to study the binding of PLAP to lipid vesicles. Sucrose-loaded vesicles were made by extrusion in 20 mM Tris, 176 mM sucrose, pH 8.1. The outside buffer was exchanged by 1:4 dilution into sucrose-free Tris-KCl buffer (20 mM Tris, 100 mM KCl, pH 8.1) and ultracentrifugation for 1 h at 100 000 g and 25 °C (Optima TLX with a TLA-100.3 rotor, 1.5 mL polyallomer microfuge tubes, Beckman Coulter, Fullerton, CA). The pelleted vesicles were resuspended in Tris-KCl buffer and used the same day. The lipid concentration was determined by the chromogenic enzyme assay. For the binding assay, sucrose-loaded POPC vesicles were diluted to concentrations ranging from 20 μ M to 10 mM. To 550 μ L of lipid suspensions we added 5 μ L of a PLAP solution of 18.6 DEA Units/mL activity in Tris-KCl buffer. After 45 min of incubation at room temperature the suspensions were centrifuged. To account for protein loss during centrifugation, tubes containing no lipid were added as a reference. The supernatant was removed as completely as possible. The enzymatic activity in the supernatant of solutions with and without lipid was determined by using *p*-NPP as a substrate. The supernatant (0.2 mL) was added to 1.8 mL of 1 mM *p*-NPP in Tris-KCl buffer and absorption over time was recorded at 405 nm. The fraction of bound phosphatase was obtained from the ratio (activity of supernatant without lipid – activity of supernatant with lipid)/activity supernatant without lipid.

Enzyme-Induced Staining of Liposomes. We studied enzymatic hydrolysis of Di-4-ASPP phosphate in the presence of large unilamellar POPC vesicles (LUVs) to observe enzyme-induced staining. Tris-NaCl Buffer was used for the preparation of all solutions. To 550 μ L of a 200 μ M solution of POPC vesicles in a cuvette was added an equal volume of Di-4-ASPP

phosphate to yield concentrations between 0.1 and 10.7 μM . PLAP (10 μL ; 18.6 DEA Units/mL) was added and the suspension was mixed by pipetting. The cuvette was held at 25 $^{\circ}\text{C}$. Fluorescence (excitation 488 nm, emission 600 nm) was recorded before and after addition of the enzyme with a resolution of 1 s. Initial velocities were determined from the slope of the first 10 to 20 s of the fluorescence traces.

Enzyme-Induced Staining of Giant Vesicles. Giant POPC vesicles were prepared by electrosweeling.^{27,28} A lipid solution (5 μL , 2 mM) in diethyl ether/methanol (9:1, v/v) was applied to a pair of planar electrodes of indium tin oxide coated with 70 nm of silica. After evaporation of the solvent under reduced pressure (0.1 mbar), 2 mL of 300 mM sucrose was added and giant vesicle formation was promoted by applying AC voltage to the electrodes. After formation was complete, vesicles were transferred to 35-mm polypropylene cell culture dishes (BD Biosciences Europe, Le Pont de Claix, France) and diluted in the same buffer. They were used the same day.

For enzyme kinetic measurements at room temperature, 400 μL of the giant vesicle stock solution was transferred to a culture dish containing 3600 μL of buffer (20 mM Tris, 100 mM NaCl, 120 mM glucose, pH 8.1). The dish had been treated overnight with poly-L-lysine (25 $\mu\text{g/L}$) to permit the immobilization of vesicles. The giant vesicles were allowed to adhere to the substrate for 15 min. Subsequently, 40 μL of a 1 mM Di-4-ASPSP phosphate solution in the same buffer was added. The fluorescence of a selected giant vesicle with a diameter of 10 to 40 μm was observed with a microscope (Axioskop, Zeiss, Oberkochen, Germany) equipped with a 100 \times water immersion objective and a b/w CCD camera (Sony ICX 285 Chip, Theta System, Gröbenzell, Germany). The light of a high-pressure mercury lamp (Zeiss) was passed through a band-pass (450/50 nm) and a dichroic mirror (505 nm). The fluorescence was detected through the dichroic mirror and a long pass filter (510 nm). Grey filters were used to reduce light intensity. The microscope was focused on the maximum diameter of the vesicles before and during the experiment. After incubation with the dye for 5 min, 40 μL of PLAP was added from a stock solution with an activity of 18.6 DEA Units/mL. Homogeneous distribution was achieved by mild pipetting. Images were recorded every 10 or 20 s before and after addition of the phosphatase. Image acquisition, camera, and shutter control as well as image analysis were performed with software written in Labview (National Instruments Germany, Munich).

Enzyme-Induced Staining of Red Blood Cells. Human erythrocytes were prepared according to a slightly modified standard procedure.²⁹ A 4-mL sample of blood from M.J.H. was sucked into a tube coated with EDTA (Vacutainer 367861, Becton Dickinson, Meylan, France) and centrifuged for 10 min at 1600 g. The pellet (~ 1 mL) was washed three times by resuspension and centrifugation for 10 min at 1600 g, using 15 mL of a 300 mOsm Tris buffer (50 mM Tris, 110 mM NaCl, pH 7.4). Finally, the pellet was diluted with an equal volume of the same buffer additionally containing 1 mM CaCl_2 . Ca^{2+} was added since it was found to increase the number of erythrocytes retaining a round shape under the experimental conditions.

The staining experiments with erythrocytes were similar to those with giant vesicles. A 2- μL sample of the erythrocyte stock solution was spread on the bottom of an untreated culture dish containing Tris buffer with CaCl_2 (20 mM Tris, 100 mM NaCl, 70 mM glucose, 1 mM CaCl_2 , pH 8.1). After 30 s, erythrocytes not adhered to the substrate were removed by washing twice. The dish was filled with 4 mL of buffer. A 1 mM Di-4-ASPSP-

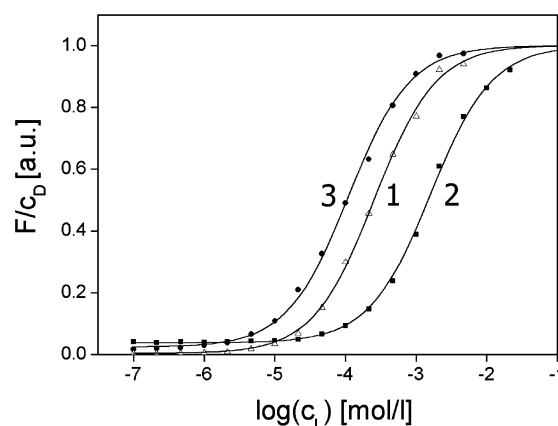


Figure 3. Fluorescence titration with lipid. The ratio F/c_D of fluorescence intensity and total concentration of dye versus the logarithm of the lipid (POPC) concentration c_L in a dispersion of lipid vesicles. The figure shows typical measurements for Di-4-ASPBS (1), Di-4-ASPSP phosphate (2), and Di-4-ASPSP alcohol (3). The data are fitted by a partitioning equilibrium with a molecular binding constant K_D and specific fluorescence intensities $f_{D,f}$ and $f_{D,b}$ of free dye in water and bound dye in lipid. For the sake of clarity, the data were normalized to $f_{D,b} = 1$ for each dye.

phosphate solution (40 μL) was added. After 5 min of incubation, 40 μL of PLAP was added from a stock solution with an activity of 18.6 DEA Units/mL. Images were taken every 30 s before and after the addition of the enzyme. To minimize UV exposure, erythrocytes were focused under red light before and, if necessary, during the experiment.

Results and Discussion

Dye Binding to Lipid. When styryl hemicyanines bind to lipid bilayers, their quantum yield of fluorescence is enhanced. Di-4-ASPBS, for example, shows a 36-fold increase in fluorescence quantum yield upon transfer from water to lecithin membranes.³⁰ We take advantage of that effect to examine the binding of Di-4-ASPSP phosphate and Di-4-ASPSP alcohol to lipid membranes by fluorescence titration.²¹ For comparison Di-4-ASPBS was also included in the investigation.

Dispersions of large lipid vesicles ($\varnothing \approx 100$ nm) were made from palmitoyl-oleoyl-phosphatidylcholine (POPC) with lipid concentrations ranging over 5 orders of magnitude. Dye was added to a concentration of 0.5 μM and fluorescence was measured. The fluorescence intensity was enhanced with increasing concentration of lipid for all three dyes as shown in Figure 3. The enhancement was shifted to higher lipid concentrations in the order Di-4-ASPSP alcohol, Di-4-ASPBS, and Di-4-ASPSP phosphate.

To evaluate the fluorescence titrations we consider a partition equilibrium of dye molecules between an aqueous and a lipid phase.²¹ With respect to the overall concentrations in the dispersion $c_{D,b}$ and $c_{D,f}$ of bound and free dye, the partition equilibrium can be expressed in terms of the lipid concentration c_L and a binding constant K_D as $c_{D,b} = K_D c_L c_{D,f}$.^{21,31} Note that this relation has the form of a mass action law, but does not imply that there is a 1:1 molecular association of dye and lipid molecules.²¹ With the total dye concentration $c_D = c_{D,b} + c_{D,f}$ we obtain eq 1.

$$c_{D,b} = \frac{1}{1 + (1/K_D c_L)} c_D \quad (1)$$

We must take into account the fluorescence of free and bound dye. With the low and high specific fluorescence intensities $f_{D,f}$

and $f_{D,b}$ of free and bound dye, the total fluorescence intensity is $F_D = f_{D,f}c_D + (f_{D,b} - f_{D,f})c_{D,b}$. Considering eq 1, it increases with the concentration of lipid according to eq 2.²¹

$$F_D = c_D \left[f_{D,f} + \frac{f_{D,b} - f_{D,f}}{1 + (1/K_D c_L)} \right] \quad (2)$$

Assuming that only the outer vesicle monolayer is stained, we use an effective lipid concentration $c_{L,eff} = c_L/2$. Asymmetry of staining was demonstrated for Di-4-ASPBS in black lipid membranes where it was a prerequisite for voltage sensitivity.³² Fits of the fluorescence data with eq 2 are shown in Figure 3. The average binding constants are $K_A = 17920 \pm 360 \text{ M}^{-1}$ for the alcohol ($n = 5$), $K_S = 7500 \pm 440 \text{ M}^{-1}$ for the sulfonate ($n = 2$), and $K_P = 1140 \pm 140 \text{ M}^{-1}$ for the phosphate ($n = 7$). The binding constant decreases when the dye bears a negatively charged headgroup.

There is an increment of the binding energy between sulfonate and alcohol of $\Delta(\Delta G_{SA}) = -RT \ln(K_S/K_A) = 2.2 \text{ kJ/mol}$ as well as for phosphate and alcohol $\Delta(\Delta G_{PA}) = -RT \ln(K_P/K_A) = 6.8 \text{ kJ/mol}$. We assign that effect to a changed resolution of the polar headgroup when the dye binds to the membrane. The polar headgroup is brought into the water/membrane interface with its lower polarity as compared to bulk water.³³ We may expect that thereby its solvation energy is reduced and that this effect is more significant for a headgroup bearing a net charge. Neglecting as a first approximation the resolution of dipoles and of higher multipoles in the headgroup, we consider the increment of resolution energy ΔG_{ion}^{resolv} of the charged moiety. We use the Born relation³⁴ for an ion of radius a and charge ze_0 that is brought from bulk water (dielectric constant $\epsilon_W = 80$) to the interfacial region with an effective dielectric constant ϵ_i according to eq 3.

$$\Delta G_{ion}^{resolv} = \frac{z^2 e_0^2}{8\pi\epsilon_0 a} \left(\frac{1}{\epsilon_i} - \frac{1}{\epsilon_W} \right) \quad (3)$$

When we identify the experimental increment of the binding energy with the Born energy as $\Delta(\Delta G_{XA}) = \Delta G_{ion}^{resolv}$, we may estimate the local polarity. For the sulfate group with $z = 1$ and $a = 0.28 \text{ nm}$ given by atomic ion radii³⁵ we obtain an effective dielectric constant $\epsilon_i = 47$ and for the phosphate with $z = 2$, $a = 0.29 \text{ nm}$, a value of $\epsilon_i = 51$. The relatively high polarities indicate a rather peripheral location of the charged groups at the membrane/water interface.³³

The number of dye molecules per unit area $n_{D,b}$ bound to the outer monolayer is determined by the concentration of free dye. Using the relation $n_{D,b} = c_{D,b}/a_L c_{L,eff}$ with the area per lipid molecule a_L we obtain eq 4, in which the free dye concentration can be expressed by the total concentration as $c_{D,f} = c_D/(1 + K_D c_L)$.

$$n_{D,b} = \frac{K_D}{a_L} c_{D,f} \quad (4)$$

For low lipid concentrations with $c_{D,f} = c_D$, staining is determined by the binding constants. At a dye concentration of $c_D = 0.5 \text{ } \mu\text{M}$ with $a_L = 0.7 \text{ nm}^2$ a rather modest staining by the alcohol would be achieved with $n_{A,b} = 1.3 \times 10^{-2} \text{ nm}^{-2}$. Enhanced staining may be expected at higher concentrations, e.g. for $c_D = 9.8 \text{ } \mu\text{M}$, the density of the alcohol would be $n_{A,b} = 0.25 \text{ nm}^{-2}$ and of the phosphate $n_{P,b} = 0.016 \text{ nm}^{-2}$. However, a high density of bound dye gives rise to weaker binding due to electrostatic repulsion in the electrical double layer.^{36,37} As

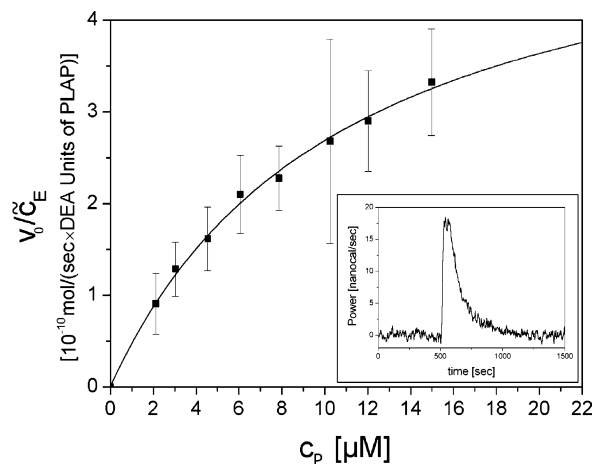


Figure 4. Enzyme kinetics by microcalorimetry. The ratio v_0/\tilde{c}_E of the initial velocity of hydrolysis and of effective enzyme concentration versus the concentration c_P of the substrate Di-4-ASPP phosphate at $25.0 \text{ } ^\circ\text{C}$. The data are fitted with Michaelis–Menten parameters K_m and \tilde{k}_{cat} . Insert: Example for a microcalorimeter tracing of reaction heat versus time after subtraction of baseline and heat of dilution ($c_P = 6.1 \text{ } \mu\text{M}$). The peak of the curve corresponds to the initial velocity. The molar heat of reaction is obtained by integration.

a test we measured the effective binding constant at a total dye concentration of $9.8 \text{ } \mu\text{M}$. The alcohol was found to have a reduced binding constant of $K_A = 8650 \pm 880 \text{ M}^{-1}$ ($n = 2$; data not shown), whereas the binding was little affected for the phosphate with $K_P = 1280 \pm 40 \text{ M}^{-1}$ ($n = 2$; data not shown).

Enzymatic Dye Hydrolysis. We tested whether Di-4-ASPP phosphate was accepted as a substrate by the soluble alkaline phosphatase from the human placenta (PLAP). After incubation with the dye, the enzyme was removed by ultrafiltration. HPLC analysis showed that Di-4-ASPP phosphate was quantitatively converted to Di-4-ASPP alcohol (data not shown). The reaction kinetics were studied by isothermal titration calorimetry (ITC). We evaluated the heat production per unit time that is proportional to the reaction rate, with the molar heat of reaction being the constant of proportionality.³⁸ The insert in Figure 4 shows the calorimeter trace of a typical measurement after the subtraction of the baseline and heat of dilution. We found that the hydrolysis was endothermal by $1.1 \pm 0.2 \text{ kJ/mol}$, a value in a typical range for monophosphoric acid esters.³⁹ By calibration with that energy, the initial reaction velocity was evaluated. The precision was limited due to the low substrate concentrations. The initial reaction velocity scaled by the effective enzyme concentration \tilde{c}_E in PLAP DEA Units/L is plotted in Figure 4 versus the substrate concentration c_P .

To evaluate the data we used Michaelis–Menten kinetics according to eq 5 with the Michaelis constant K_m , an effective maximum rate constant \tilde{k}_{cat} per DEA Units of PLAP, and an effective enzyme concentration \tilde{c}_E .

$$-\frac{dc_P}{dt} = \frac{\tilde{k}_{cat}\tilde{c}_E}{1 + (K_m/c_P)} \quad (5)$$

We fitted the initial velocity $v_0 = -(dc_P/dt)_0$ by nonlinear regression and obtained $K_m = 10.9 \pm 4.3 \text{ } \mu\text{M}$ and $\tilde{k}_{cat} = 0.56 \pm 0.12 \text{ nmol/s Units}$ ($n = 3$). The hydrolysis is slow compared to $\tilde{k}_{cat} = 17 \text{ nmol/s Units}$ for the common model substrate *p*-nitrophenyl phosphate (*p*-NPP) at optimal conditions (pH 9.8, $37 \text{ } ^\circ\text{C}$, DEA buffer). However, the reaction conditions with pH 8.1, $25 \text{ } ^\circ\text{C}$, Mg^{2+} -free, chosen for stability of vesicles and cells, are quite different. Under these conditions, the rate constant for *p*-NPP hydrolysis was $\tilde{k}_{cat} = 0.35 \text{ nmol/s Units}$ (data not

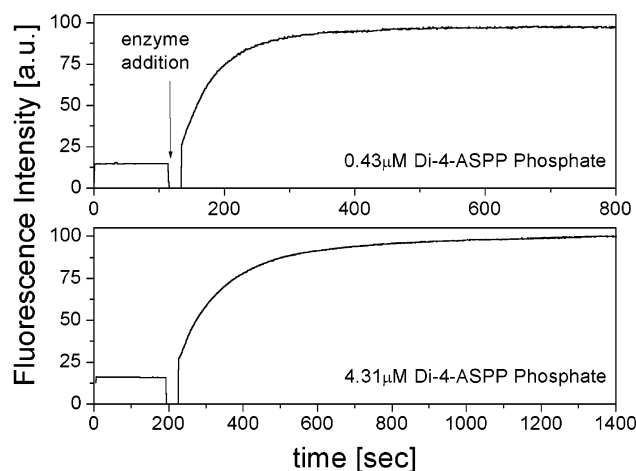


Figure 5. Enzyme-induced staining of the lipid membrane. Fluorescence intensity versus time of a vesicle suspension (lipid concentration 100 μM POPC) at two concentrations 0.43 (top) or 4.31 μM (bottom) for the substrate Di-4-ASPP phosphate. The addition of phosphatase is marked by an arrow.

shown). We conclude that Di-4-ASPP phosphate is accepted by PLAP as a regular substrate.

Enzyme-Induced Staining of Liposomes. Now, we combined the two previous experiments. The dye phosphate was hydrolyzed by phosphatase in the presence of lipid vesicles. The reaction was observed by the enhancement of fluorescence due to the enhanced binding of the dye alcohol to the lipid. Two examples are shown in Figure 5. The fluorescence intensity of a vesicle suspension (100 μM lipid) was recorded before and after the addition of the phosphatase with 0.43 and 4.31 μM Di-4-ASPP phosphate. It was enhanced about 6-fold from a low level caused by the binding of the substrate to a high level caused by binding of the product. This corresponds to the ratio of the fluorescence lipid titration data of alcohol and phosphate at 100 μM lipid (cf. Figure 3 and eq 2). We conclude that staining of lipid membranes is accomplished by enzymatically induced enhancement of lipophilicity.

We attempted a quantitative evaluation of time-dependent fluorescence in terms of the Michaelis–Menten kinetics of hydrolysis coupled to equilibrated water/lipid distribution of substrate and product. Both dyes contribute to the total fluorescence, proportional to their concentrations c_P and c_A with $c_{\text{tot}} = c_P + c_A$ according to eq 2. We denote the total fluorescence of the suspension before and after the reaction by F_0 for $c_P = c_{\text{tot}}$ and by F_∞ for $c_P = 0$. During the reaction the fluorescence is $F(t) = F_0[c_P(t)/c_{\text{tot}}] + F_\infty[1 - c_P(t)/c_{\text{tot}}]$ and the initial velocity of the reaction is obtained from the initial slope of intensity according to eq 6.

$$v_0 = \frac{c_{\text{tot}}}{F_\infty - F_0} \left(\frac{dF}{dt} \right)_0 \quad (6)$$

Using eq 6, we evaluated the kinetic data for vesicle suspensions of 100 μM POPC with 0.17 DEA Units/mL of PLAP in a concentration range of Di-4-ASPP phosphate from 0.1 to 10.7 μM . The initial velocities v_0 are plotted versus the dye concentration in Figure 6. From a fit of the data by eq 5 we obtained $K_m = 7.3 \pm 0.6 \mu\text{M}$ and $\tilde{k}_{\text{cat}} = 0.53 \pm 0.2 \text{ nmol/s Unit}$ ($n = 3$).

There is good agreement between the enzyme kinetic parameters obtained by the fluorescence measurements in a lipid suspension and those obtained by ITC in a lipid free solution.

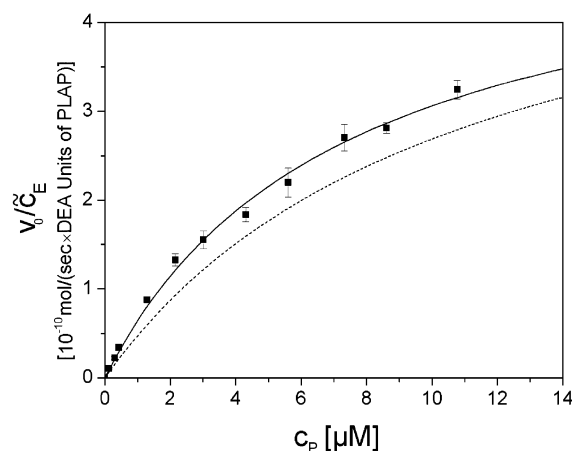


Figure 6. Enzyme kinetics by fluorometry in a vesicle suspension. The ratio v_0/\tilde{c}_E of the initial velocity of hydrolysis and of the effective enzyme concentration versus concentration c_P of the substrate Di-4-ASPP phosphate at a lipid concentration of 100 μM (25.0 $^\circ\text{C}$). The data are fitted with Michaelis–Menten parameters K_m and \tilde{k}_{cat} . The fit obtained from microcalorimetric experiments (Figure 4) is indicated as a dashed line.

However, several problems have to be considered in a quantitative evaluation of the enzyme reaction with lipid vesicles by indirect observation of fluorescence: (i) Do we observe a hydrolysis by free or by lipid bound enzyme? (ii) Do we observe a hydrolysis of free or of lipid bound substrate? (iii) Does binding of the dye to the enzyme contribute to enhanced fluorescence? (iv) Is there an effect caused by changed electrostatics during the reaction—with negatively charged membrane before and positively charged membrane after the reaction? (v) Is there an interference caused by the flip-flop dynamics of the product across the membrane? To consider these questions, we performed additional experiments.

(i) **Lipid-Bound Enzyme.** We checked whether PLAP interacts with POPC membranes using a sucrose-loaded vesicle binding assay. PLAP was incubated with sucrose-filled liposomes. After incubation, the liposomes and potentially bound PLAP were removed by ultracentrifugation, and the percentage of bound PLAP was calculated from the residual enzymatic activity of the supernatant. Commonly, this assay yields sigmoidal binding isotherms for proteins,²⁶ similar to fluorescence lipid titration. With PLAP, the assay indicated that between 8% and 20% of the protein were removed by ultracentrifugation (Figure 7A). There was no significant dependence of the fraction of bound enzyme on the lipid concentration. We conclude that the observed binding is an artifact introduced by the assay and that there is no specific binding of the enzyme to the vesicles, i.e., that we observe dye hydrolysis by free enzyme.

(ii) **Lipid-Bound Substrate.** We examined whether the reaction rate depends on the fraction of bound substrate that increases with the lipid concentration according to eq 1 (Figure 7B, dashed line). We evaluated the fluorescence kinetics with 0.5 μM Di-4-ASPP phosphate at various lipid concentrations as shown in Figure 7B (squares). The reaction rate slows down inversely to the fraction of bound dye. We conclude that the membrane-bound dye phosphate is not accessible to the phosphatase. In the kinetic experiments described above, this inhibiting effect was avoided by using a low lipid concentration of 100 μM .

(iii) **Enzyme-Bound Dye.** The initial fluorescence F_0 of enzyme kinetics was measured prior to the addition of enzyme, while the fluorescence increase and the final fluorescence F_∞ were obtained in the presence of enzyme. When we added PLAP to a solution of the product Di-4-ASPP alcohol, the fluorescence

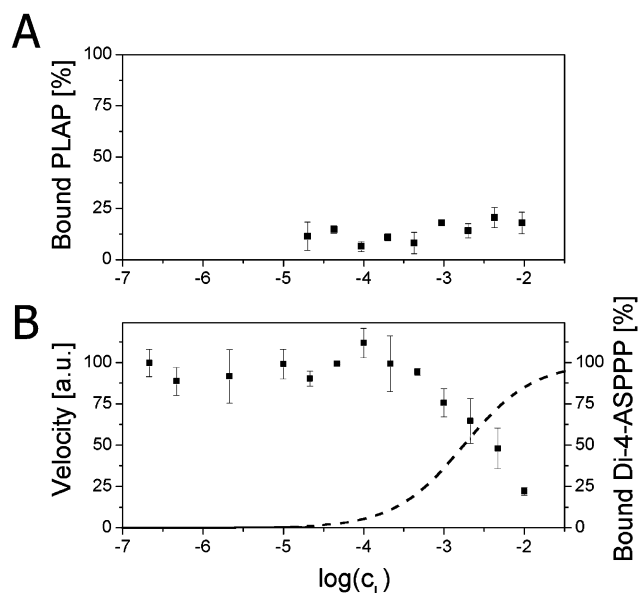


Figure 7. Perturbation of enzyme kinetics by the lipid-bound enzyme and the lipid-bound substrate. (A) Percentage of bound enzyme PLAP versus lipid concentration determined by a sucrose-loaded vesicle binding assay. The fraction of bound phosphatase is not significant considering the accuracy of the method (see text). (B) Reaction rate of enzymatic hydrolysis of Di-4-ASPP phosphate versus lipid concentration. For comparison, the fraction of lipid-bound substrate as calculated by eq 1 is plotted as a dashed line.

of the solution increased due to an enhanced fluorescence quantum yield of dye bound to the surface of protein. We found that a protein concentration of 0.17 DEA Units/mL of PLAP corresponded to a lipid concentration of around 5 μM from experiments in the presence of both lipid and PLAP (data not shown). Thus at the lipid concentration of 100 μM , the effect of dye binding to the protein can be neglected.

(iv) *Electrostatics.* During the course of the reaction, the surface potential of the liposomes changes from a low negative value due to weakly bound phosphate to a higher positive value due to bound alcohol. Considering eq 4 the effect leads to a lower binding constant at high dye concentrations and a sublinear increase of fluorescence with hydrolysis. The role of the phosphate is negligible due to its low binding constant. The effect of alcohol affects the maximum fluorescence F_∞ used in the evaluation of the initial reaction velocity. Considering the good match of fluorescence assay and ITC data, we did not consider that effect.

(v) *Flip-Flop.* In the kinetic measurement at the high dye concentration of 4.31 μM in Figure 5, bottom, the fluorescence does not level out at a constant F_∞ but grows with a small constant slope. The effect was observed for dye concentrations above 3 μM . It may be attributed to a slow flip of the dyes to the inner monolayer of the liposome and enhanced binding. The effect was not apparent at lower dye concentrations, because the fluorescence increase due to reaction was much faster than the increase due to flip-flop. In the evaluation of the data, we defined F_∞ by the fluorescence at the time where constant slope was attained.

The discussion of problems i to v indicates that adequate enzyme and lipid concentrations must be chosen in the fluorescence assay with liposomes to obtain data that reliably reflect enzyme activity in the aqueous phase. Some error may be introduced by electrostatics and flip-flop. Nonetheless, the fluorescence assay can be used as a reliable and sensitive method to test novel enzymatically activated amphiphilic dyes.

Enzyme-Induced Staining of Giant Vesicles. As a first example for enzyme-induced staining of a cell-like system, we chose giant lipid vesicles ($\varnothing \approx 10\text{--}40\ \mu\text{m}$). Individual vesicles of POPC were incubated with 9.8 μM of the dye phosphate and observed in a microscope with a CCD camera. Figure 8A shows a sequence of images before and after the addition of the phosphatase. Apparently, the fluorescence of the membrane increases considerably after addition of the enzyme. Figure 8A impressively demonstrates that enzyme-induced staining is possible with individual cell-like structures.

We evaluated the intensity of a row of pixels of the image at the maximum diameter in the y-direction as shown in Figure 8B. A plot of intensity minus background versus time is shown for three different vesicles in Figure 8C. The fluorescence intensity was normalized to the maximum value for each experiment. After addition of the enzyme the fluorescence increased from a constant low value F_0 caused by staining with the phosphate to a high constant value F_∞ due to staining by the alcohol. The ratio of intensities was $F_\infty/F_0 = 9\text{--}13$.

The fluorescence intensity in a microscope that is focused on the membrane is dominated by membrane-bound dye, i.e., by the density of bound dye molecules $n_{D,b}$ with little contribution of the solution. $n_{D,b}$ is determined by the concentration of free dye according to eq 4 where we may assume $c_{D,f} \approx c_D$ since the number of giant vesicles in the culture dish was very small and hence the solution was not depleted. Considering eq 4, we expect that the ratio of fluorescence intensity before and after the staining process is solely determined by the ratio of the binding constants of the dyes, if excitation and recording of fluorescence are identical for phosphate and alcohol. For liposome suspensions, we measured $K_A/K_P \approx 16$ at low dye concentrations and $K_A/K_P \approx 7$ at a concentration of 9.8 μM . The ratio of the fluorescence intensities $F_\infty/F_0 = 9\text{--}13$ found with giant vesicles is in good agreement.

During the reaction, the fluorescence is $F(t) = F_0[c_P(t)/c_{\text{tot}}] + F_\infty[1 - c_P(t)/c_{\text{tot}}]$. We compute the dynamics of the normalized fluorescence F/F_∞ by inserting the Michaelis–Menten dynamics (eq 5) and integrating it with the parameters determined by ITC. The result is plotted in Figure 8C (dashed line). The perfect agreement with the data shows that staining of giant vesicles is indeed due to enzymatic activation of the precursor dye.

Enzyme-Induced Staining of Erythrocyte Membrane. The plasma membrane of cells consists of a variety of charged and uncharged lipids and of membrane proteins. It is well-known that voltage-sensitive dyes are able to bind to membrane proteins.⁴⁰ Therefore it must be checked whether an enzyme-induced change of headgroup polarity leads to increased staining of a eucaryote membrane. In test experiments with nerve cells we observed fast endocytosis and staining of intracellular membranes for the dyes used in our study. For that reason we chose erythrocytes as a model. Red blood cells have a rather inactive plasma membrane and no internal organelles.

Di-4-ASPP phosphate was added to human erythrocytes attached to a culture dish to a concentration of 9.8 μM . Membrane fluorescence was measured in the same setup as with giant vesicles. Fluorescence was weaker than with giant vesicles, which we attribute to fluorescence quenching by hemoglobin and the smaller size of the erythrocytes. Figure 9A shows an example of a sequence of images of the erythrocyte membrane before and after addition of phosphatase. The fluorescence intensity significantly increased. The experiment proves that the enzyme-induced modulation of headgroup polarity is an effective mechanism of staining also with cell membranes.

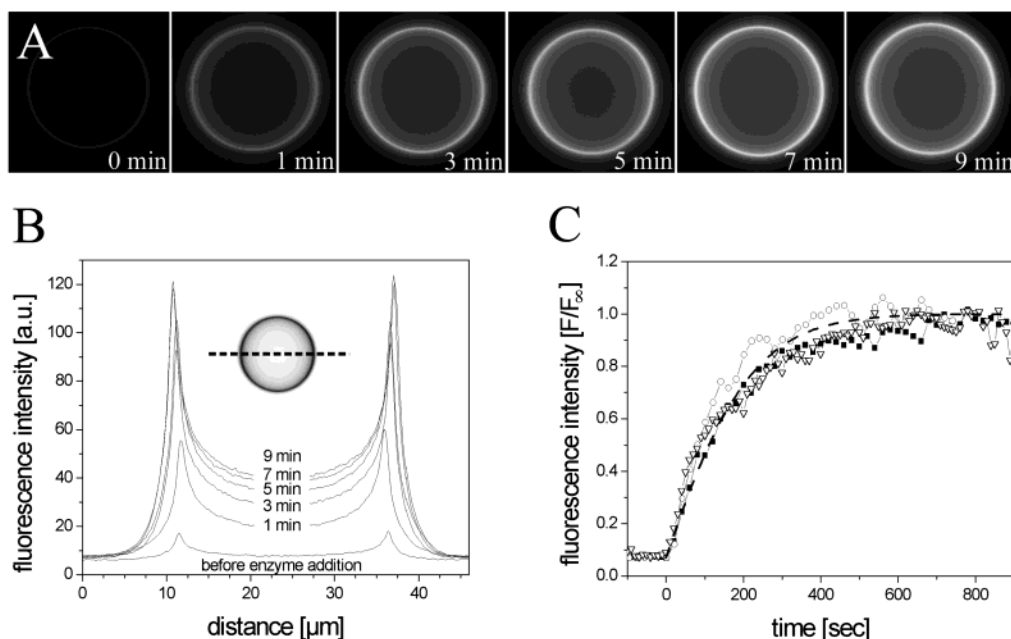


Figure 8. Enzyme-induced staining of a giant lipid vesicle. (A) Fluorescence image (excitation around 450 nm, emission at >510 nm) of a giant vesicle before (0 min) and after addition of phosphatase (activity 0.18 DEA Units/mL). Di-4-ASPSP phosphate was present at a concentration of $9.8 \mu\text{M}$. (B) Profiles of fluorescence intensity across the diameter (approximately $27 \mu\text{m}$) of a vesicle. (C) Normalized fluorescence intensity of the vesicle membrane (peak of the profile minus background) versus time for three different vesicles. The dashed line is the fluorescence computed with the enzyme kinetic parameters K_m and \bar{k}_{cat} from ITC and a scaling factor of fluorescence fitted to the data.

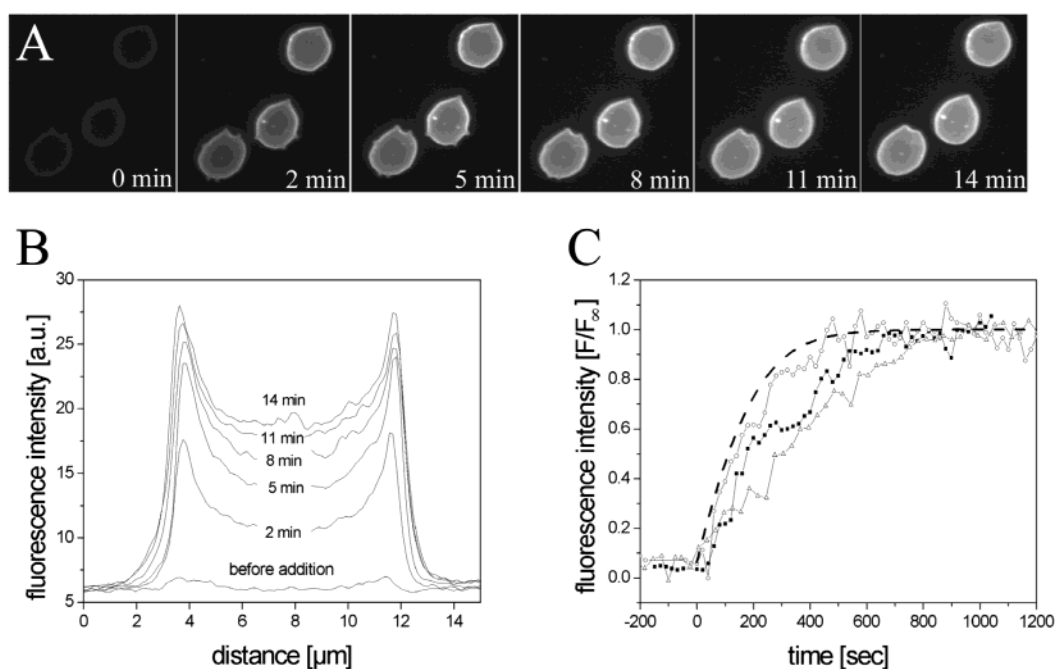


Figure 9. Enzyme-induced staining of the erythrocyte membrane. (A) Fluorescence image (excitation around 450 nm, emission at >510 nm) of an erythrocyte before (0 min) and after addition of phosphatase (activity 0.18 DEA Units/mL). Di-4-ASPSP phosphate was present at a concentration of $9.8 \mu\text{M}$. (B) Profiles of fluorescence intensity across the diameter of an erythrocyte with a diameter of about $8 \mu\text{m}$ on the culture dish. (C) Normalized fluorescence intensity of the vesicle membrane (peak of the profile minus background) versus time for three different vesicles. The dashed line is the fluorescence computed with the enzyme kinetic parameters K_m and \bar{k}_{cat} from ITC and a scaling factor of fluorescence fitted to the data.

Plots of the intensity of a row of pixels cutting through the image of an erythrocyte at its maximum diameter are shown in Figure 9B. The normalized maximum brightness minus the background signal versus time is shown in Figure 9C. The ratio of final and initial fluorescence was $F_{\infty}/F_0 = 11\text{--}25$ with an average of 15. These values are similar to the fluorescence enhancement on giant vesicles. Also the fluorescence dynamics

during staining that is computed from the Michaelis–Menten kinetics agrees fairly well with the experiments as shown in Figure 9C. However, the variation of the experiments and the deviation from the expected reaction progress is larger than that for giant vesicles. We think that there is a larger experimental error due to the weaker fluorescence and due to changes of shape of the erythrocytes during the measurement.

Conclusion

In the present paper we proposed a new concept for selective staining of membranes and cells with voltage-sensitive dyes. The underlying principle is to increase the binding strength of the dye to membranes by enzymatic cleavage of a functional group that impairs binding. The work presented provides the physicochemical fundament for that staining mechanism. In addition, it implies a method for screening dyes, functional groups, and enzymes for future developments. The crucial issues to be considered in the future are (i) a development of dye pairs with a larger difference of resolution energies upon membrane binding, (ii) an application of better voltage-sensitive chromophores that do not permeate a cell membrane such as ANNINE dyes,^{9,10} (iii) the transfection of eucaryotic cells with membrane-bound enzymes suitable for dye hydrolysis, and (iv) the development of functional groups that are susceptible to enzymes not endogenous in nerve tissue.

Acknowledgment. We thank Michaela Morawetz, Sonja Golla, and Stephanie Stumhofer for excellent technical assistance, Christian Figger for expert LABVIEW programming, Armin Lambacher for technical advice on fluorescence spectroscopy and quasidynamic light scattering, Elisabeth Weyher-Stingl for performing the HPLC analysis of the phosphatase, and Monika Sommer for taking the blood samples.

References and Notes

- (1) Tasaki, I.; Watanabe, A.; Sandlin, R.; Carnay, L. *Proc. Natl. Acad. Sci. U.S.A.* **1968**, *61*, 883.
- (2) Cohen, L. B.; Salzberg, B. M.; Davila, H. V.; Ross, W. N.; Landowne, D.; Waggoner, A. S.; Wang, C. H. *J. Membr. Biol.* **1974**, *19*, 1.
- (3) Cohen, L. B.; Salzberg, B. M. *Rev. Physiol. Biochem. Pharmacol.* **1978**, *35*.
- (4) Loew, L. M.; Bonneville, G. W.; Surow, J. *Biochemistry* **1978**, *17*, 4065.
- (5) Loew, L. M.; Simpson, L. L. *Biophys. J.* **1981**, *34*, 353.
- (6) Fluhler, E.; Burnham, V. G.; Loew, L. M. *Biochemistry* **1985**, *24*, 5749.
- (7) Grinvald, A.; Hildesheim, R.; Farber, I. C.; Anglister, L. *Biophys. J.* **1982**, *39*, 301.
- (8) Grinvald, A.; Fine, A.; Farber, I. C.; Hildesheim, R. *Biophys. J.* **1983**, *42*, 195.
- (9) Hübener, G.; Lambacher, A.; Fromherz, P. *J. Phys. Chem. B* **2003**, *107*, 7896.
- (10) Kuhn, B.; Fromherz, P. *J. Phys. Chem. B* **2003**, *107*, 7903.
- (11) Bullen, A.; Saggau, P. Optical Recording from Individual Neurons in Culture. In *Modern Techniques in Neuroscience Research*, 1st ed.; Johansson, H., Ed.; Springer: Berlin, Germany, 1999; p 89.
- (12) Sinha, S. R.; Saggau, P. Optical Recording from Populations of Neurons in Brain Slices. In *Modern Techniques in Neuroscience Research*, 1st ed.; Johansson, H., Ed.; Springer: Berlin, Germany, 1999; p 459.
- (13) Grinvald, A.; Shoham, D.; Shmuel, A.; Glaser, D.; Vanzetta, I.; Shtoyerman, E.; Slovov, H.; Wijnbergen, C.; Hildesheim, R.; Arieli, A. In *Vivo Optical Imaging of Cortical Architecture and Dynamics*. In *Modern Techniques in Neuroscience Research*; Johansson, H., Ed.; Springer: Berlin, Germany, 1999; Vol. 1, p 893.
- (14) Grinvald, A.; Salzberg, B. M.; Lev-Ram, V.; Hildesheim, R. *Biophys. J.* **1987**, *51*, 643.
- (15) Antic, S.; Zecevic, D. *J. Neurosci.* **1995**, *15*, 1392.
- (16) Siegel, M. S.; Isacoff, E. Y. *Neuron* **1997**, *19*, 735.
- (17) Sakai, R.; Canonigo, V. R.; Raj, C. D.; Knöpfel, T. *Eur. J. Neurosci.* **2001**, *13*, 2314.
- (18) Massoud, S. S.; Sigel, H. *Inorg. Chem.* **1988**, *27*, 1447.
- (19) Georgatos, J. G. *Arch. Biochem. Biophys.* **1967**, *121*, 619.
- (20) Hassner, A.; Birnbaum, D.; Loew, L. M. *J. Org. Chem.* **1984**, *49*, 2546.
- (21) Fromherz, P.; Röcker, C. *Ber. Bunsen-Ges. Phys. Chem.* **1994**, *98*, 128.
- (22) Gregoriadis, G. *Liposome Technology*; Vol. 1, Preparation of Liposomes; CRC: Boca Raton, FL, 1984; Vol. 1.
- (23) MacDonald, R. C.; MacDonald, R. I.; Menco, B. P. M.; Takeshita, K.; Subbarao, N. K.; Hu, L. R. *Biochim. Biophys. Acta* **1991**, *1061*, 297.
- (24) Eriksson, H. J. C.; Somsen, G. W.; Hinrichs, W. L. J.; Frijlink, H. W.; de Jong, G. J. *J. Chromatogr. B* **2001**, *755*, 311.
- (25) Grit, M.; Crommelin, D. J. *Chem. Phys. Lipids* **1993**, *64*, 3.
- (26) Buser, C. A.; McLaughlin, S. *Methods Mol. Biol.* **1998**, *84*, 267.
- (27) Dimitrov, D. S.; Angelova, M. I. *Bioelectrochem. Bioenerg.* **1988**, *253*, 323.
- (28) Fromherz, P.; Kiessling, V.; Kottig, K.; Zeck, G. *Appl. Phys. A* **1999**, *69*, 571.
- (29) Schwoch, G.; Passow, H. *Mol. Cell. Biochem.* **1973**, *2*, 197.
- (30) Ephardt, H.; Fromherz, P. *J. Phys. Chem.* **1989**, *93*, 7717.
- (31) Heerklotz, H.; Seelig, J. *Biochim. Biophys. Acta* **2000**, *1508*, 69.
- (32) Fromherz, P.; Schenk, O. *Biochim. Biophys. Acta* **1993**, *1191*, 299.
- (33) Fernández, M. S.; Fromherz, P. *J. Phys. Chem.* **1977**, *81*, 1755.
- (34) Born, M. *Z. Phys.* **1920**, *1*, 45.
- (35) Shannon, R. D. *Acta Crystallogr. A* **1976**, *32*, 751.
- (36) McLaughlin, S. *Curr. Top. Membr. Transp.* **1977**, *9*, 71.
- (37) Tan, A.; Ziegler, A.; Steinbauer, B.; Seelig, J. *Biophys. J.* **2002**, *83*, 1547.
- (38) Todd, M. J.; Gomez, J. *Anal. Biochem.* **2001**, *296*, 179.
- (39) Tewari, Y. B.; Steckler, D. K.; Goldberg, R. N.; Gitomer, W. L. *J. Biol. Chem.* **1988**, *263*, 3670.
- (40) Visser, N. V.; van Hoek, A.; Visser, A. J.; Frank, J.; Apell, H. J.; Clarke, R. J. *Biochemistry* **1995**, *34*, 11777.